Dev Genes Evol (2006) 216: 667–681
DOI 10.1007/s00427-006-0094-3

ORIGINAL ARTICLE

Albert Cardona · Volker Hartenstein · Rafael Romero

Early embryogenesis of planaria: a cryptic larva feeding on maternal resources

Received: 28 February 2006 / Accepted: 21 May 2006 / Published online: 24 August 2006

Abstract The early planarian embryo presents a complete ciliated epidermis and a pharynx and feeds on maternal yolk cells. In this paper, we report on all the elements involved in the formation of such an autonomous embryo, which we name cryptic larva. First, we provide a description of the spherical and fusiform yolk cells and their relationship with the blastomeres, from the laying of the egg capsule up to their final fate in mid embryonic stages. Then, we describe the early cleavage and the subsequent development of the tissues of the cryptic larva, namely, the primary epidermis, the embryonic pharynx, and a new cell type, the star cells. Finally, we discuss the possibility that the cryptic larva either constitutes a vestigial larva or, more likely, is the evolutionary result of the competition between multiple embryos for the limited and shared maternal resources in the egg capsule.

Keywords Flatworm · Planaria · Embryogenesis · Larva · Competition

Introduction

Planarians have become a favorable group of animals to study embryonic development and regeneration in the same model system (Sanchez-Alvarado 2003; Cardona et al. 2005a). As members of the phylum Platyhelminthes, planarians occupy a phylogenetic position at the base of the Lophotrochozoa (Baguna and Riutort 2004). They exhibit a combination of derived and simple features, the latter thought to be shared with the common bilaterian ancestor. Historically, the scarcity of external morphological landmarks, in conjunction with a relatively slow life cycle, has hindered the exploration of planarians as a model in developmental biology. The tools of molecular biology have more recently enabled the researcher to monitor the expression of genes and proteins (Umesono et al. 1997), knockout genes temporarily by RNAi (Sanchez Alvarado and Newmark 1999; Bueno et al. 2002; Reddien et al. 2005), and to identify cell types and tissues molecularly (Bueno et al. 1997; Cardona et al. 2005a). These tools were brought to bear on questions of regeneration, as well as of axis formation and questions of cell fate (Cardona et al. 2005a). The renewed interest in planarian development necessitates detailed developmental studies. In this paper, we report on the structure and development of the peculiar feeding stage that characterizes the early *Schmitdea* embryo.

Early embryonic development of planarians exhibits several fundamental characteristics that deviate from the standard mode of spiral cleavage from which it most likely derives (Thomas 1986). Planarian eggs are ectolecithal, meaning that the yolk-poor oocytes are surrounded by a mantle of specialized yolk cells (vitellocytes; for a review, see Benazzi and Gremigni 1982). A single egg or egg capsule typically contains multiple (one to nine in *Schmitdea*) oocytes. As cleavage starts, yolk cells in the vicinity of zygotes fuse into a local syncytial domain around the cleaving blastomeres. Blastomeres do not remain attached to each other to form a compact morula but instead spread out throughout the yolk syncytium and only secondarily join up to form the embryonic primordium (Koscielski 1966). At an early stage, a subset of blastomeres assembles and differentiates into a motile, yolk-feeding organism that resembles in many respects a larval form. The early planarian embryo was indeed called 'larva' by previous authors (Fulinski 1916; Seilern-Aspang 1958; Koscielski 1966); we will use the term "cryptic larva" in the following. The cryptic larva possesses a complete epidermis, a pharynx, and a number of neuron-like cells; it moves freely within the

Communicated by D.A. Weisblat

A. Cardona (✉) · V. Hartenstein
Molecular Cell and Developmental Biology,
University of California Los Angeles,
621 Charles E. Young Drive South,
Los Angeles, CA 90095, USA
e-mail: cardona@ucla.edu

A. Cardona · R. Romero
Facultat de Biologia, Departament de Genètica,
Universitat de Barcelona,
Diagonal 645,
08028 Barcelona, Spain

egg capsule and pumps the non-fused, spherical yolk cells into its interior which thereby develops into the gastric cavity. As the cryptic larva grows and acquires a gut cavity, the syncytial yolk and the blastomeres enclosed within it are compressed into a thin peripheral rind. Within this rind, blastomeres proliferate and differentiate into the various tissues of the juvenile worm. By contrast, the cells of the cryptic larva itself are only transient; they are totally resorbed and substituted by definitive tissues during mid-embryonic stages (le Moigne 1963; Cardona et al. 2005a).

In this paper, we focus on the morphogenetic processes that give rise to the cryptic larva. First, we have analyzed yolk structure and development, as many questions in regard to the involvement of yolk cells in early embryogenesis are unanswered. Then, we describe in detail the tissues of the cryptic larva and the subset of blastomeres that give rise to them. We discuss the different ways to interpret the cryptic larva in the phylogenetic context, either as a vestigial larva that evolved from a true larval form or as an adaptation to the intraspecific competition set up by the occurrence of multiple zygotes in a single egg capsule.

Materials and methods

Animals and egg capsules

Egg capsules were collected daily from a laboratory culture of *Schmidtea polychroa* (diploid strain from Sot de Ferrer, Castell, Spain). The animals were fed with raw sheep liver twice a week.

Electron microscope preparations

The egg capsules were perforated with the help of a 0.5-μm needle and fixated in 4% paraformaldehyde, 2.5% gluteraldehyde in 0.1 M phosphate buffer (PB, pH 7.3; freshly made from 10% of 0.2 M $NaHPO_4$, 40% of 0.2 M $NaHPO_4$, and 50% H_2O) for 24 h. The egg capsules were then rinsed 5×10 min in 0.1 M PB, and then the embryos were dissected under the microscope. The desired embryos were then postfixed in 1% osmium tetraoxyde in 0.2 M PB for 60 min at 4°C and then rinsed 4×10 min in H_2O. Dehydration was done through acetone series (10 min 50%, 10 min 70%, 10 min 96%, and 3×10 min 100%). Embedding in Spurr's (10 g ERL 4206, 6 g DER 736, 26 g NSA, 0.4 g DMAE S-1, and 0.8 g DBP; mixed in this order) was done at room temperature as: 2 h 1:3 Spurr to acetone, 3 h 2:2, overnight 3:1, 2 h Spurr, overnight Spurr, and finally 48 h in Spurr at 60°C for polymerization. Both semithin and ultrathin sections were obtained from blocks. The ultrathin sections were mounted on gold grids and counterstained with uranyl acetate and lead citrate. Semithin sections were mounted on gelatin-coated slides and counterstained with methylene–toluidine blue, then mounted in Spurr under a cover glass.

Scanning electron microscope preparations

The embryos were fixed and dissected as described above for electron microscopy. After fixative rinse, the embryos were dehydrated in an alcohol series (50, 70, 96, and 2×100%) and then transferred to amyl acetate. The embryos were subsequently dried by means of CO_2 critical point drying and then coated with gold–palladium.

Whole-mount preparations

Whole-mount immunostainings and sytox nuclei labeling were prepared as described in Cardona et al. (2005a).

In situ hybridization

In situ hybridization was performed in paraffin sections as described in Cardona et al. (2005b). The probe for the *myoD* gene was synthesized from a clone containing 1,264 bp corresponding to the complete cDNA for the *Schmidtea mediterranea* gene (Cebrià 2000). The riboprobes were labeled with UTP-digoxygenin using the in vitro Roche labeling kit.

Microscopy and image processing

Optical microscopy images were taken with an Axiophot (Zeiss) microscope. The confocal stacks were taken with a Biorad2000. A JEOL 1010 transmission electronic microscope attached to a Bioscan (Gatan) digitalization station and a Zeiss DSM 940 A scanning electronic microscope were used. The images were processed in ImageJ (Rasband 2005), and the figures were assembled in Photoshop (Adobe).

Three-dimensional modelling

The custom ImageJ (Rasband 2005) plug in "3D Editing" was used (http://www.pensament.net/java/) to outline all structures in two dimensions and calculate the three-dimensional skins. Then data were imported into Blender (Blender Foundation) and colored and rendered by ray tracing.

In vitro embryo and yolk cell culture

Whole egg capsules were rinsed 3×15 min in autoclaved culture water, in 50-ml tubes filled up to 40 ml, and submitted to rotation in an orbital shaker. For each rinse, the egg capsules were placed in a sterile Petri dish and picked up manually with tweezers for transfer to the next 50-ml tube, under tissue culture conditions. For yolk cell culture, the egg capsules were bathed for 5 min in SDS-saturated autoclaved culture water and then rinsed 4×5 min under shaking

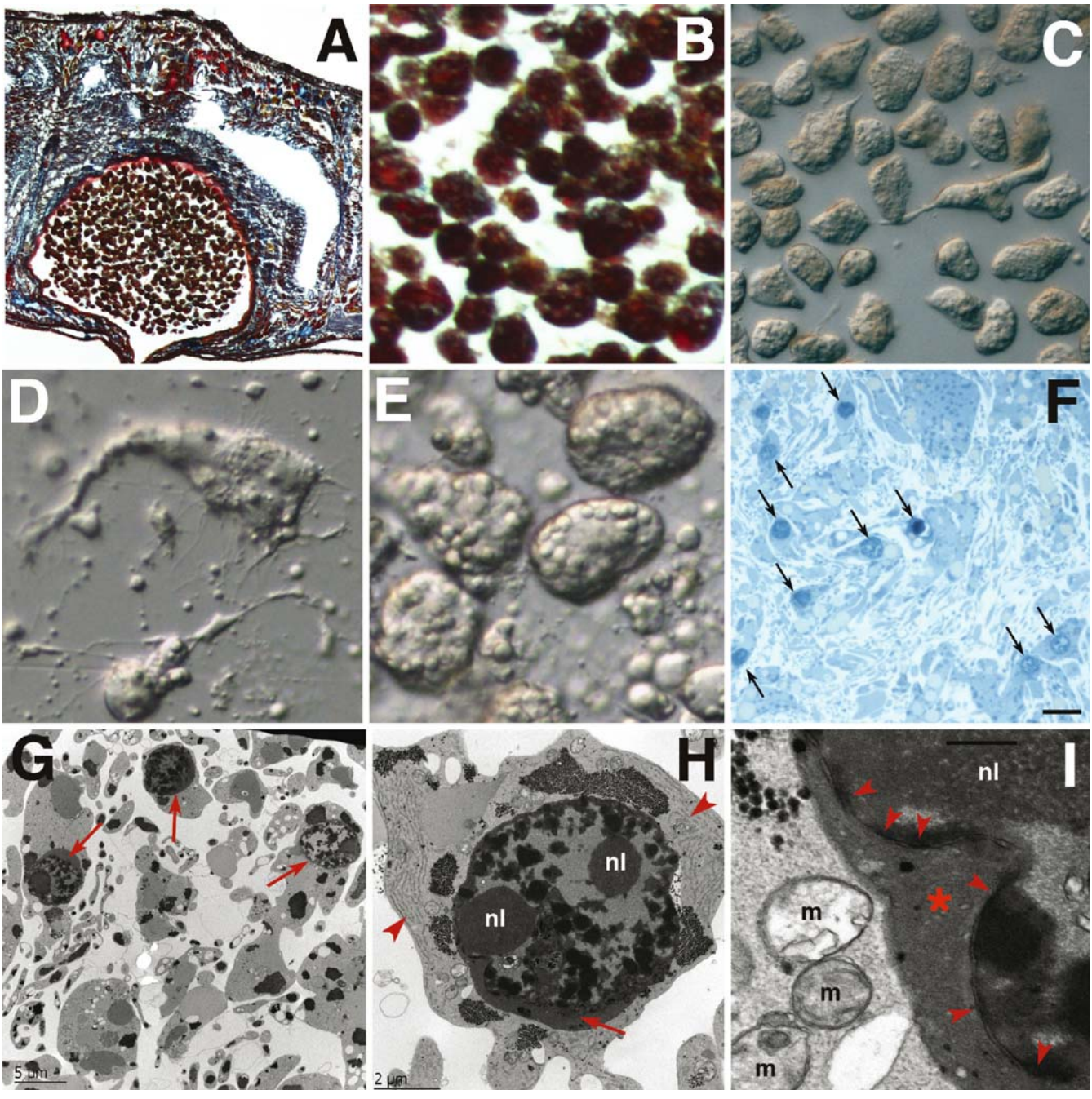

Fig. 1 Vitellocytes at day 0. **a**, **b** Mallory staining; **c**, **d** live cell spread; **f** semithin section stained with MTB; **g**–**i** transmission electronic microscopy. **a** Sagittal section of an adult individual showing the atrium with an egg capsule in the process of being formed. *Large hollow white* spaces are gut diverticula. **b** Higher magnification of the yolk cells contained in the forming egg capsule in **a**. Note all cells present a spherical shape. **c** Live day 0 yolk cells. Most present a roughly spherical morphology. **d** Higher magnification of a fusiform yolk cell. Note the many fine cytoplasmic processes. **e** Spherical vitellocytes present numerous oil and yolk granules within the cytoplasm; note the presence of free granules outside the cells. **f** Vitellocytes (*arrows* point to all visible nuclei), beside their yolk content, present numerous cytoplasmic projections, visible as sectioned profiles. There are no appreciable differences among vitellocytes. **g** The nucleus of each vitellocyte (*red arrows*) contains a large nucleolus and clumps of condensed chromatin. The cytoplasmic projections contain mainly clumps of glycogen rosettes (*dark profiles*). **h** The cytoplasm of the vitellocyte contains large clumps of glycogen rosettes (*dark profiles*), mitochondria (*small gray profiles*), and numerous sacs of endoplasmic reticulum (*arrowheads*). The nucleus is wrapped by a corona of electron-dense material (*arrow*) and contains two large nucleoli (*nl*) and numerous clumps of chromatin. **i** High magnification of a vitellocyte nucleus. The cytoplasm, *left*, contains several mitochondria and glycogen rosettes (*top left*). The double membrane of the mitochondrial crista (*m*) is visible, indicating a good fixation. The corona (*asterisk*) is composed of a fibrillar electron-dense material; glycogen rosettes can be found within (*dark profiles*). The nuclear envelope presents numerous pori complexes (*arrowheads*). The nucleus, *right*, contains a huge nucleolus (*nl* at *top*, partially visible as granulous material) and very electron-dense clumps of chromatin. *Scale bars* 10 µm in **f**, 5 µm in **g**, 2 µm in **h**, and 0.1 µm in **i**

conditions. For early stages of development, whole egg capsules were subsequently transferred to a Petri dish containing 5% low-gelling point agarose (Sigma) in Leibovitz medium (Gibco) supplemented with 10% foetal calf serum (Gibco). The egg capsule was then broken and removed with the help of a sharp needle and tweezers under the microscope; the high viscosity of the medium prevented the curling shell from damaging the embryos. For the culture of embryos in the late stages, 5% agarose in plain autoclaved water was used. The Petri dishes containing specimens were then cooled at 4°C for 5 min, for the agarose to harden, and then kept parafilm-sealed at 17°C.

Results

Yolk cells and syncytium formation

Yolk cells or vitellocytes are produced in a set of specialized maternal glands, the vitellaria. They are then delivered to the atrium where they assemble around the oocytes and become enclosed by a hardening egg shell (Domenici and Gremigni 1974). At this stage, all vitellocytes represent a homogenous population of spherical cells packed with lipid granules (Fig. 1a,b). Vitellocytes present a spherical morphology as well when extracted from the eggshell immediately after egg laying (ref. Fig. 1c).

Within the first day after egg laying, a second type of yolk cell becomes apparent which is elongated and possesses multiple fine, filopodia-like processes (Fig. 1d); this type differs qualitatively from the round, yolk-laden (spherical) cells (Fig. 1e). The fusiform yolk cells were already described by Marinelli and Vagnetti (1973). Domenici and Gremigni (1974) assumed that fusiform yolk cells differentiate from spherical yolk cells in response to unknown stimuli from within the egg. The presence of free yolk granules within yolk cells (Fig. 1d,e) supports their hypothesis. During the second and third day after egg deposition, the fusiform cell type represents a major fraction of yolk cells within the egg capsule (Fig. 1f). Fusiform yolk cells are distributed throughout the egg capsule and are not restricted to the neighborhood of oocytes, as suggested by previous works (Seilern-Aspang 1958; Koscielski 1966). Fusiform yolk cells ultrastructurally show heterochromatin-rich, round nuclei surrounded by a peculiar corona of electron-dense, hyaline material (Fig. 1g,h) which contains a variety of membranous organelles, yolk granules (not shown), and glycogen rosettes (Fig. 1i). A similar corona, although not explicitly denoted as such, is visible in the figure material of a previous report on yolk cells by Marinelli and Vagnetti (1973, their Fig. 3). The nucleus of fusiform yolk cells contains one or two large nucleoli (Fig. 1h), suggesting a high level of activation.

During cleavage of the zygote (stage 1, days 1–2), fusiform yolk cells fuse into a syncytium that envelops the blastomeres (Fig. 2a). We have observed a row of vesicles that possibly indicates the line of membrane fusion between yolk cells, particularly those of the yolk-cell-derived hull membrane (data not shown), suggesting that fusion occurs simultaneously at many points of the yolk cell cytoplasmic membrane. A layer of yolk cells surrounding the growing syncytium also join up to form a thin sheet, called hull membrane, around the yolk (Fig. 2a, asterisk). The syncytial cytoplasm is rich in lipid droplets, yolk granules, and clumps of glycogen rosettes (Fig. 2a,b). The syncytial yolk nuclei maintain their ultrastructural characteristics, including the distinctive hyaline corona that contrasts sharply with the granular cytoplasm of the surrounding syncytium (Fig. 2c,d). It is interesting to note that mitotic figures are frequent among syncytial yolk nuclei within the stage 2 embryo (Fig. 2e–g,i). The fact that, when present, a large fraction of the syncytial nuclei were in mitosis suggests some degree of synchronization.

According to the classical literature, syncytial yolk cell nuclei are, at least in part, resorbed during relatively early stages (le Moigne 1963; Koscielski 1966); on the other hand, the possibility that they could persist and become cellularized was also suggested (le Moigne 1969). We have observed intact syncytial yolk nuclei scattered among embryonic cells within the germ throughout stages 3 and 4 of development (Fig. 2j,k). The fact that syncytial yolk nuclei undergo division and remain undisrupted until the onset of stage 5 suggests that they play an active and

Fig. 2 The syncytium. **a**, **e**–**i** acTub-labeled (*brown*) semithin sections counterstained with MTB. **b**–**d**, **j**, **k** Electron microscopy images. **a** Early stage 2. The syncytium contains numerous oil droplets (*yellow profiles*) and syncytial yolk nuclei (*dark blue profiles*). The syncytium is not yet fully enclosed within the primary epidermis cells; in this section, the top is still in continuity with fused yolk cells that will be sliced off (*asterisk*). Yolk cells either not fused or sliced off from the syncytium form a yolk-derived hull membrane that traps the expanding primary epidermis cells within a tight space (*red arrow*). The primary epidermis cells are barely visible at this magnification (*black arrow*). **b** Three syncytial yolk nuclei (*arrows*) presenting the typical corona and clumps of condensed chromatin. The syncytium is very rich in oil droplets (*large gray profiles*) and glycogen (*dark agglomerations*). **c** The principal subset of syncytial nuclei presents a light nucleus (*n*) with a large nucleolus (*nl*), and their corona (*asterisk*) is very homogeneous. **d** Detail of the lower right vesicle in **c**. The membrane of the vesicle is clearly visible (*arrows*), in opposition to the limit of the corona (*arrowhead*), which presents none. Rough endoplasmic reticulum (*lower right*). The *black spots* are glycogen rosettes. **e** Partial view of the stage 2 syncytium. Two mitotic figures (*small arrowheads*) are visible along a syncytial nucleus (*white arrow*) and a blastomere (*large arrowhead*), which lays in a visible cleft (an artifact due to paraformaldehyde fixation). The primary epidermis is ciliated (*ci*) and labeled with acTub. **f**, **g**, **i** Detail of mitotic figures among syncytial nuclei. Note the typical corona presented by these nuclei, hosting the mitotic figure in *F* and *I*. **h** higher magnification of a blastomere. The cytoplasm of all blastomeres is strongly labeled with acTub (*n*, nucleus). **j**, **k** Stage 4 germ band. **j** Two syncytial nuclei within the germ band. A nucleolus (*nl*) is visible, and the general nuclear appearance has not changed substantially since stage 2, suggesting that these nuclei are still active. The cytoplasm of the syncytial germ band contains oil droplets and abundant glycogen rosettes (*dark spots*). **k** A blastomere derivative. Note the multilobed nucleus with two large nucleoli (*nl*; one, in the *top right* lobe, barely visible in this section). Many membranous structures populate the cytoplasm (to the *right*). In the adjacent syncytium, hundreds of mitochondria (*white profiles*) line the cell. The primary epidermis (*pe*) is greatly flattened. *Scale bars* 5 μm in **b**, 0.3 μm in **c**, 0.2 μm in **d**, 20 μm in **e**

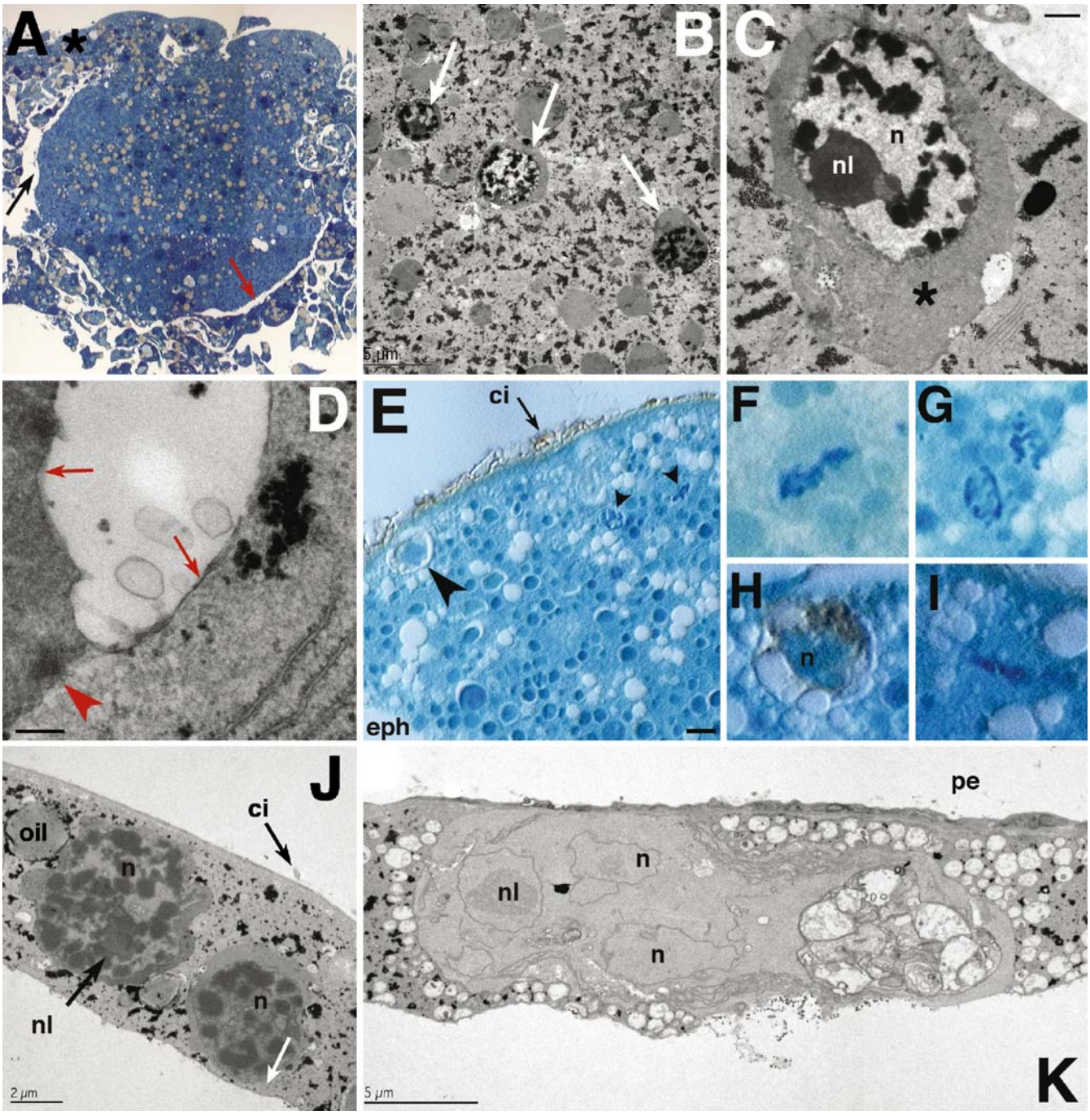

important role in the syncytium and thus in the early embryonic events.

The structure and development of blastomeres

During early cleavage, blastomeres impose as large cells (15–25 µm) with multilobulated nuclei, containing two to three large nucleoli and electron-lucent chromatin (Fig. 3a–c; Cardona et al. 2005a). Nuclei are often accompanied by electron-dense particles near the nuclear membrane, which could be interpreted as chromatoid bodies (an organelle composed by RNA and proteins including VASA and PL10-like helicases; Auladell et al. 1993; Shibata et al. 1999; Orii et al. 2005; Fig. 3c,e). Gap junctions are apparent between the membrane of blastomeres and the syncytium (Fig. 2d). On the syncytial side of the membrane, a conspicuous network of cortical actin filaments surrounds the blastomeres (Fig. 3i). These cytoskeletal fibers could be instrumental in anchoring the dense population of mitochondria to the syncytial cortex surrounding the blastomeres (Fig. 3d).

There are about 15–20 blastomeres within a stage 2 embryo. At this early stage, the blastomeres express tyrosinated tubulin (Fig. 3h); a subset reacts to anti-serotonin and anti-acetilated tubulin (see Fig. 7). Many blastomeres also express the gene *myoD* (Fig. 3f,g). As the embryonic

pharynx starts functioning and pumps yolk into the interior of the embryo (stage 3), the blastomeres become organized into a loose layer that fills the syncytium. By late stage 3, approximately 100–200 *myoD*-expressing blastomeres can be recognized (Fig. 3j). As division continues, the blastomeres subsequently decrease in size and change their ultrastructural characteristics, transforming into the various types of embryonic precursor cells that differentiate shortly thereafter (Cardona et al. 2005a). The embryonic precursor cells of a stage 4 embryo have an irregular, lobulated shape, with electron-lucent nuclei that lack chromatoid bodies (Fig. 2k). A large fraction still expresses *myoD* (Fig. 3j,k), which possibly signifies their later fate as myocytes; by contrast, other early markers of blastomeres, including acetylated tubulin and serotonin, are no longer expressed, further demonstrating that a differentiation process has occurred between cleavage and stage 4.

Formation of the primary epidermis

A fraction of blastomeres are set aside at an early stage of cleavage to differentiate into the various cell types of the cryptic larva, which include the primary epidermis, embryonic pharynx, and the star cells; the latter might constitute a small population of transient neurons. The primary epidermis consists of a single layer of ciliated, flat cells that wrap the yolk syncytium and the cleaving blastomeres contained therein, thereby delimiting the embryo from the surrounding external yolk cells (le Moigne 1963; Cardona et al. 2005a). The primordium of the primary epidermis can be first seen at early stage 2 as a small population of contiguous flattened cells adjacent to the primordium of the embryonic pharynx (Fig. 4a). The primordia of the primary epidermis and embryonic pharynx seem to be closely related not only spatially but also in terms of the cellular markers they express. Both express tyrTub (Cardona et al. 2005a), as well as the small cysteine-rich protein TNEX-59, during their initial stages of differentiation (Fernández-Rodríguez, unpublished data).

During the course of stage 2, the primordium of the embryonic epidermis extends out from the embryonic pharynx towards the opposite pole in a process described as "reverse epiboly" (Fig. 4a–c; reviewed in Thomas 1986). The primary epidermal cells contact the underlying yolk syncytium by means of putative gap junctions (Fig. 4d,e). The advancing primary epidermis appears to push its way through the yolk syncytium (Fig. 4c,f). Thus, one frequently observes vacuoles in the syncytium, ahead of the leading edge of the primary epidermis (Fig. 4f), suggestive of a mechanism in which the advancing cells actively intrude and thus "slice off" part of the syncytium. The yolk outside the primary epidermis forms a thin layer, the yolk-cell-derived hull membrane (Cardona et al. 2005a). This membrane has to be manually dissected for the study of stage 2 embryos. The remnants of the hull membrane can still be found in stages 3 and 4 embryos (not shown).

The primordium of the primary epidermis at early stage 2 includes approximately 20 cells. This number does not increase significantly during later stages. The conclusion that proliferation of primary epidermal cells is rare, if it occurs at all, is confirmed by the absence of mitotic figures within the primary epidermis at any stage in histological material or preparations labeled with anti-phosphohistone (not shown). The use of colchicine in embryos taken out of the egg capsule and cultured in vitro caused apoptosis (not shown), which hindered the observation of mitotic figures among primary epidermis cells.

Fig. 3 Blastomeres. **a**, **b** Semithin sections stained with MTB. **c**–**e** Transmission electronic microscopy images. **f**, **g**, **j**, **k***myoD* in situ hybridization on paraffin sections. **h**–**j** z-projection of confocal stacks of whole-mount preparations; **h** of tyrTub (*red*); **i** actin fiber bundles in the stage 2 embryo syncytium; nuclei in *green*. **a** A late stage 2 or earliest stage 3 embryo. The embryonic pharynx has not yet started imbibing yolk cells but wide spaces are being opened within the syncytium (*top*). On both sides of the pharynx, two undefined masses of material (*asterisks*) accumulate, which will be visible until the resorption of this organ. Several blastomeres are visible in the syncytium (*arrows*); one presents very large vesicles within (*red arrow*). The primary epidermis completely wraps the syncytium and is thicker nearby the embryonic pharynx (*top left arrowhead*) and opposite to it (*bottom right arrowhead*). **b** Higher magnification of a blastomere from **a**. The wide and multilobed nucleus (*n*) contains three nucleoli (*large dark blue profiles within*), typically adjacent to the nuclear envelope. The surrounding syncytium is very rich in vesicles of all kinds, indicating a high level of activity. **c** A blastomere similar to that in **b**. The nucleus (*light gray*) has many lobes and contains two visible nucleoli. Putative chromatoid bodies are present as *tiny dark spots* adjacent to the nuclear envelope (see **e**). The cytoplasm contains three visible and very typical large vacuoles (*white spaces within*). This blastomere lays adjacent to the embryonic pharynx external envelope (*top left*). **d** detail of **c**. The cytoplasm of the blastomere (*right*) is rich in free ribosomes. Mitochondria (*m*) lying on the syncytium line the blastomere, as seen at lower magnification in **c**. Both the syncytial and the blastomeric cytoplasmic membranes are visible (*arrowheads*) and contact each other by putative GAP junctions (*arrow*). The *dark spots* within the syncytium are glycogen rosettes. **e** Higher magnification of the *top right* nucleolus in **c**, displaying the typical non-electron-dense center. A putative chromatoid body is shown on the lower left (*dark spot*) in close association to the nuclear envelope. **f** Stage 2. *myoD* is expressed in most cells of the embryonic pharynx (*eph*) and also in all or in a subset of the blastomeres (*top*), which typically lie in their own vacuoles (stressed artefactuously by paraformaldehyde). Syncytial yolk nuclei are completely negative. **g** Two cells with a similar morphology to stage 2 blastomeres expressing *myoD* in the germ band of stage 3 embryo. These embryos present up to 40 of such cells. **h** The blastomeres present a very dense and polarized network of microtubules, as revealed by tyrTub. The blastomeric nucleus has such a low density that the Sytox labeling is barely visible in it. The other *strong green* nuclei are presumably syncytial yolk nuclei, showing the typical clumps of condensed chromatin. **i** Long stretches of actin bundles appear to be connecting some blastomere-containing vesicles with each other. A layer of actin defines the vesicle in which each blastomere is enclosed. Actin filaments bundle and sprout from the layer that wraps the nucleus, providing an explanation for the clustering and retention of high numbers of mitochondria nearby each blastomere (see **d**). Many syncytial nuclei (smaller, *free of red* coating) are also visible (as *small green profiles*). What appears to be the blastomeres' cytoplasmic actin (in *yellow*, on the *right*) is an artifact generated by the z-flattening of the confocal stack. **j** Stage 3 and **k** stage 4 *myoD* expression on embryo paraffin sections. The *panels* are to scale with each other. Only a subset of the total number of embryonic cells is labeled, which amounts to about 300 cells in the stage 3 embryo when summing counts for all slices. *Scale bars* 25 μm in **a**, **f**; 5 μm in **b**, **c**; 0.5 μm in **d**, **e**; 10 μm in **g**; 20 μm in **h**, **i**; and 200 μm in **j**, **k**

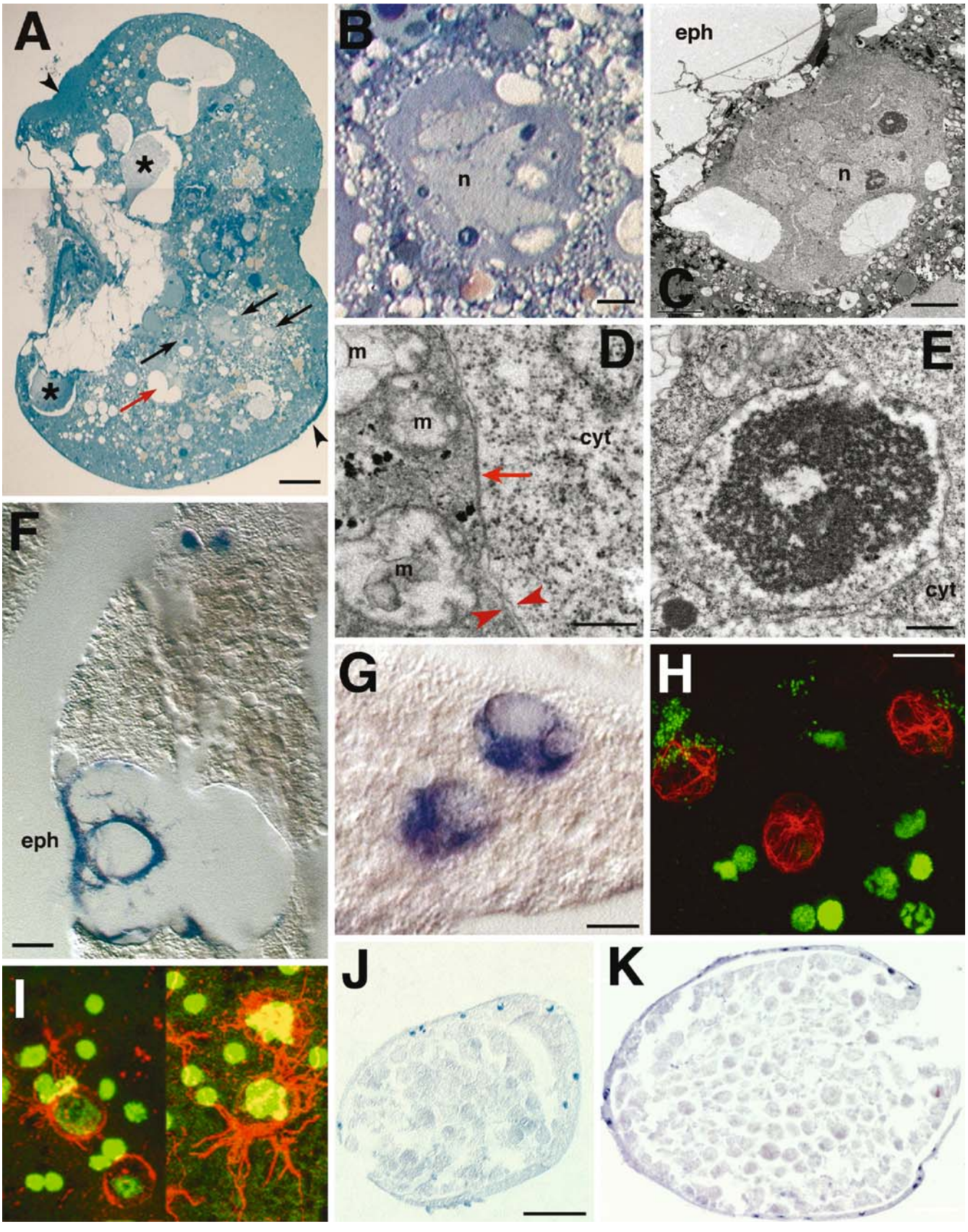
A
B
n
eph
n
C
m
D
m
cyt
m
E
cyt
F
eph
G
H
I
J
K

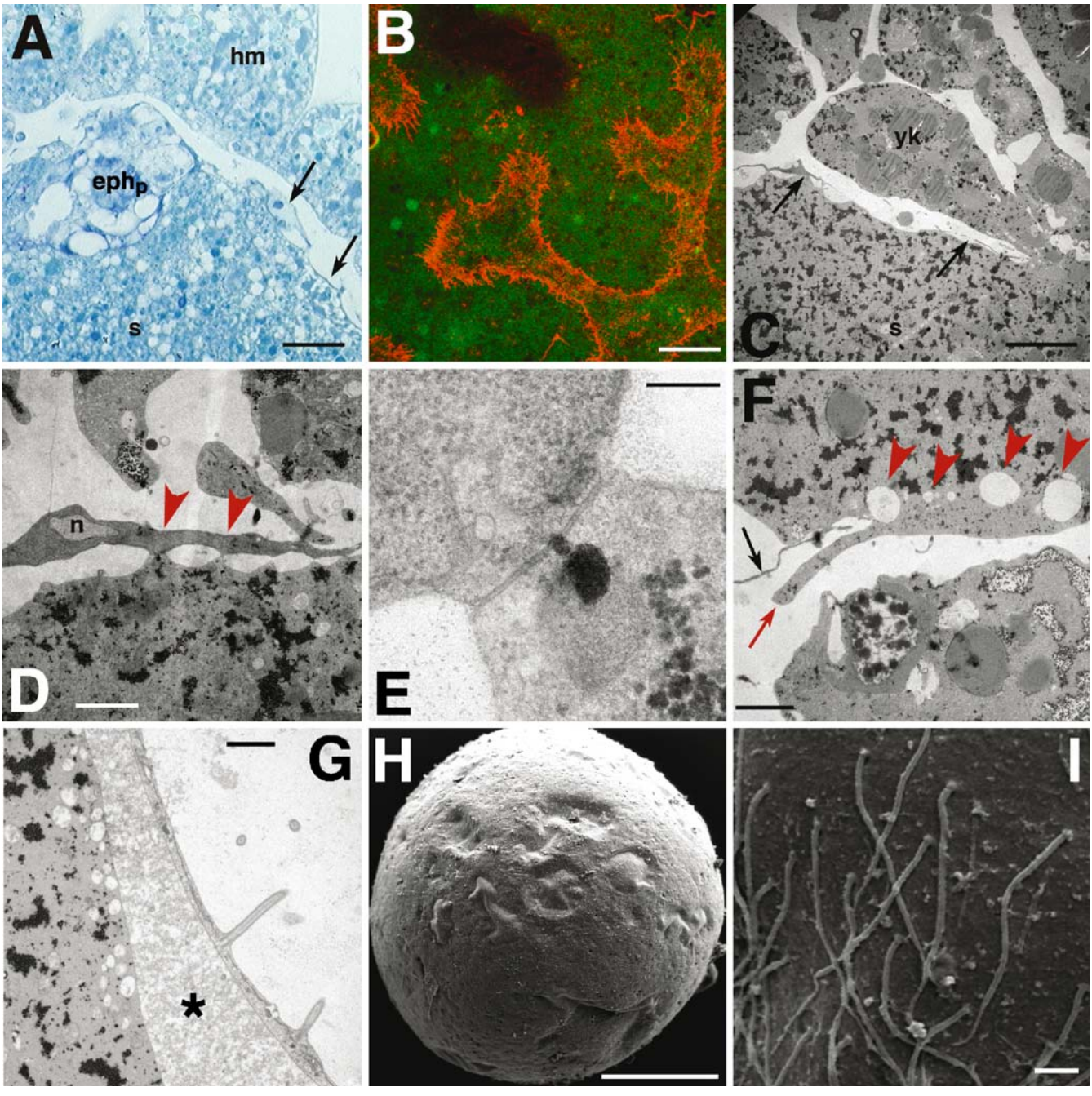

Fig. 4 Primary epidermis. **a** Semithin section stained with MTB. **b** Confocal z-projection of anti-actin-labeled whole mount. **c**–**g** Transmission electronic microscopy images. **h**, **i** Scanning electronic microscopy images. **a** As the embryonic pharynx primordium (*eph*) grows and differentiates at one edge of the syncytium (*s*), several cells escape and develop into a continuous layer, the pioneers of the primary epidermis (*arrows*). External yolk cells line the outside of the embryo, making a yolk-cell hull membrane (*hm*). **b** Surface view of a stage 2 embryo, showing primary epidermis cells (in *red*) with spiky edges. **c** Embryonic epidermis cells extend thin sheets (*arrow*) that either slice off part of the syncytium (*lower part*, *s*) or prevent external yolk cells (*yk*) from fusing completely. **d** Early primary epidermis cell (*n*, nucleus) contacts the syncytial surface at discrete points (*red arrows*). These early primary epidermis cells, lacking both a basement membrane and tight junctions, may be homologous to the hull membrane of macrostomids. **e** Higher magnification of an epidermal cell contact with the syncytium, showing a putative gap junction. **f** Embryonic epidermal cell (*arrow*) penetrating the syncytium. Within the syncytium, several vesicles are present at what looks like the prospective path of the penetrating embryonic epidermal cell. The sliced-off area (*red arrow*) is distinctively poorer in glycogen and other reserve materials. **g** Late stage 2 embryo presenting a flattened ciliated primary epidermis. Between the syncytium and the embryonic epidermis, an unknown material accumulates (*asterisk*), which will be later on compacted into a basement membrane. The syncytium is still rich in glycogen (*black profiles*, *left*). **h** Late stage 2 embryos are completely ciliated and show no evident ciliary bands or tufts. **i** High magnification of stage 2 embryo in **h**. Cilia present thickened ends where they meet the surface of the embryonic epidermis. *Scale bars* 20 μm in **a**, **b**; 10 μm in **c**; 2 μm in **d**; 0.2 μm in **e**; 3 μm in **f**; 1 μm in **g**, **i**; and 100 μm in **h**

By the end of stage 2, a large portion of the yolk syncytium, containing most if not all of the blastomeres produced up until that stage, is encapsulated in a continuous epithelial sheet. There is initially no basement membrane, and primary epidermis cells contact the syncytial membrane directly at discreet points, possibly by gap junctions (Fig. 4d,e). By contrast, no cell–cell contacts are established with the outer yolk cells or the yolk-cell-derived hull membrane (Fig. 4c,d), suggesting that the primary epidermal cells are already polarized at this stage. As the embryo progresses through stage 2, the primary epidermis cells differentiate. Cilia and microvilli appear at their apical surface (Fig. 4g–i). A loose basement membrane is secreted in between the syncytial surface and the basal surface of the primary epidermis (Fig. 4g), which gets compacted through stage 3 (Fig. 5a–c). Intercellular junctions form in between neighboring epidermal cells (Fig. 6h,i). Compared to the ciliation of the definitive epidermis of the juvenile, that of the primary epidermis is sparse (Figs. 4g–i and 5a–c). The primary epidermal cilia are rather irregularly spaced and significantly shorter (about 6 μm) than the cilia of the juvenile epidermis (about 18 μm). No trochophore-like bands or tufts of cilia are visible. At some locations, notably near the embryonic pharynx, the primary epidermis adopts a double-layered configuration (Fig. 1a), and ciliation is denser than elsewhere (Fig. 6h).

As the embryo enters stage 3 and starts imbibing yolk, the primary epidermis and its basement membrane stretch and become thinner (Fig. 3j,k; Fig. 5a–c) and will ultimately be substituted by a second wave of epidermis formation during stage 5 (le Moigne 1963; Tyler and Tyler 1997; Cardona et al. 2005a,b).

The older literature (Fulinski 1916) speculated on the existence of an inner epithelium at the interface of the imbibed yolk cells and the syncytium, which would derive from the embryonic gut, a structure made of four cells laying on the inner end of the embryonic pharynx (le Moigne 1963). Our electron microscopic data do not reveal any epithelial layer separating the imbibed yolk cells from the syncytium (Fig. 5d,e).

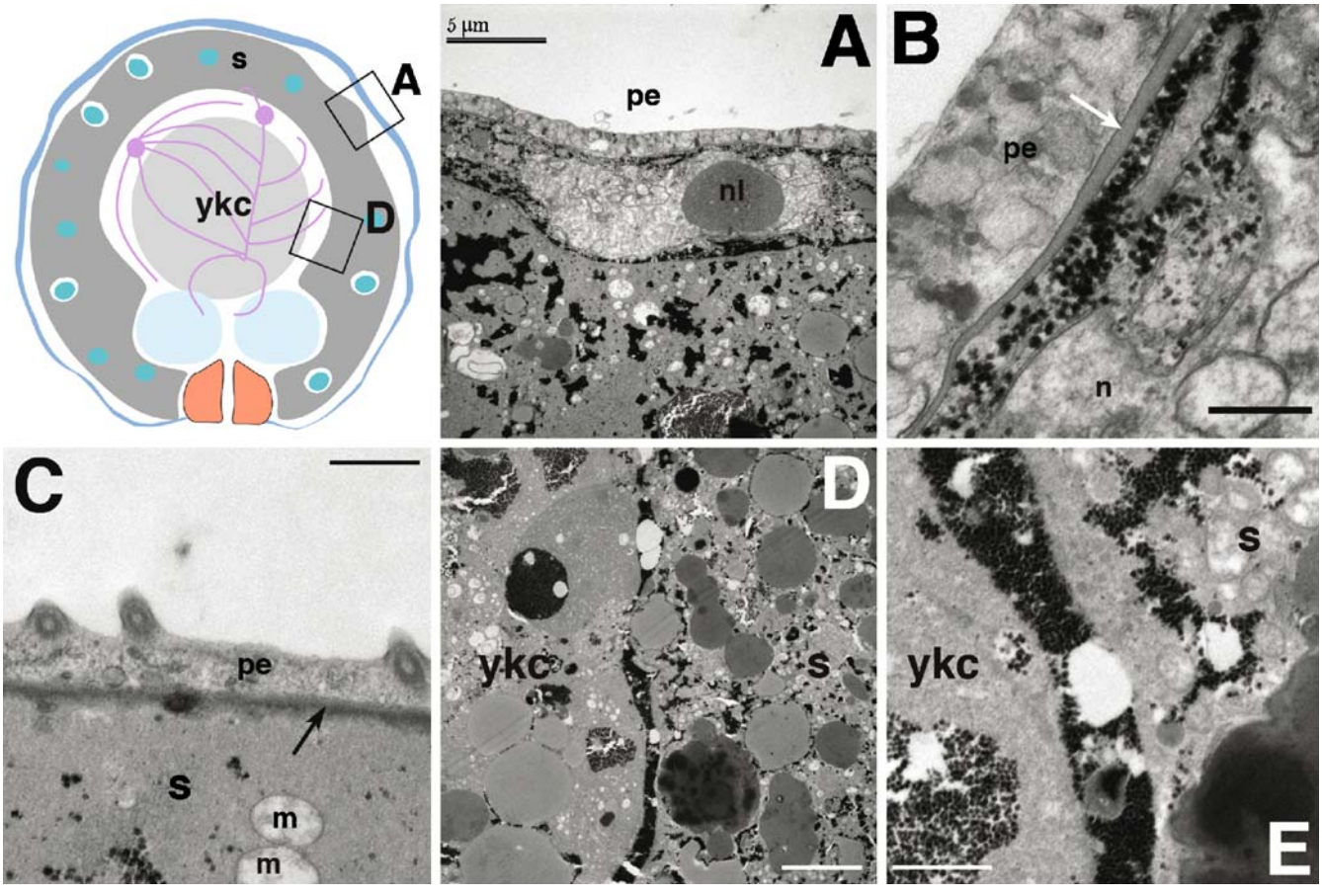

Fig. 5 Transmission electronic microscopy images of stage 3 embryos. **a** Surface of the embryo. A cell can be found outside the syncytium, underneath the embryonic epidermis, presenting a nucleus (*white profile*) with a huge nucleolus (*nl*). **b** Detail of **a**. The primary epidermis cells (*pe*) contain numerous organelles and lay on a basement membrane (*arrow*; *n*, nucleus). **c** The primary epidermal cells are ciliated and separated from the syncytium by a basement membrane (*arrow*). **d** The limit (*vertical black line*) between ingested yolk cells (*left*, *ykc*) and the syncytium (*right*, *s*) presents no conspicuous cells. **e** Detail of **d**, the limit of the yolk cells and the syncytium. No cells are present. A mass of glycogen rosettes fills this extracellular space. *Scale bar* 5 μm in **a**, **d**; 0.5 μm in **b**, **c**; and 0.5 μm in **e**. *s*, syncytium; *m*, mitochondrium. The extracellular spaces are cluttered with glycogen rosettes (*black dots*)

The embryonic pharynx

The transient pharynx of the cryptic larva ("embryonic pharynx"; le Moigne 1963) is formed during stage 2 from a population of prematurely differentiating blastomeres (Stevens 1904; le Moigne 1963; Koscielski 1966; Cardona et al. 2005a); persisting until stage 5, it is eventually replaced by the definitive pharynx of the juvenile. The embryonic pharynx comprises epithelial, muscular, nervous, and glandular cells and serves the purpose of pumping external vitellocytes into the embryo. A cluster of blastomeres giving rise to these tissues appears at the beginning of stage 2 and defines the posterior pole of the embryo (Fig. 4a).

The lumen of the embryonic pharynx is lined by four epithelial cells surrounded by circular muscle fibers (Fig. 6a; le Moigne 1963). The radial muscle fibers connect the inner tubular structure with an outer epithelial sheet (Fig. 6a,c,d). Small anti-serotonin-labeled cells are present thorough the entire embryonic pharynx, possibly forming part of a pharyngeal nervous plexus (Fig. 5b). Large, seemingly empty spaces lie in between the radial muscle fibers (Fig. 6d,e). It is not clear whether these spaces correspond to large vacuoles within a syncytial mass or they are extracellular in nature. The presence of conspicuous cell membranes (Fig. 6e) juxtaposed to the membranes of radial muscle fiber cells supports the former, but further investigations are necessary to clarify this point. At the base of the pharynx, the epithelium that faces the exterior of the cryptic larva is heavily ciliated (Fig. 6h,i).

Fig. 6 Embryonic pharynx. **b** z-projection of a confocal stack showing anti-serotonin labeling. **c**–**i** Transmission electronic microscopy images. **a** 3D model of the embryonic pharynx. Lateral view, the opening is *down*, not visible. Note the particular disposition of circular and radial muscle fibers (*green*) around the central lumen (*red*). The external envelope is rendered as a wireframe for clarity. **b** Whole mount of a stage 2 section showing anti-serotonin labeling in the embryonic pharynx (*eph*) and in a collection of blastomeres. No star cells are visible on this side of the embryo. **c** Cross-section of the embryonic pharynx. The lumen (*asterisk*) is filled with a vitellocyte (note its nucleus to the right of the *asterisk*). The epithelial layer that defines the lumen (*dark gray band*) is continuous with the two big masses (to the *right*), which are most likely the main parts of the cellular bodies. A band of circular muscle (*light gray*) wraps the inner epithelium, and radial muscle fibers have their bodies (*arrow*) attached to the circular muscle. **d** Detail of **c**. The circular muscle fibers are very thin (*light gray band*, *arrow*). The cellular body of a radial muscle fiber presents a light nucleus with a central nucleolus. **e** The embryonic pharynx is contained within an epithelial envelope, a cell of which is shown here containing numerous endoplasmic reticulum sacs and organelles, as well as glycogen rosettes. The cell sits on a basement membrane (*arrowhead*) not facing the syncytium but the spaces among the radial muscle fibers (*top left*) of the pharynx. The presence of an extra membrane below the basement membrane suggests that the inner spaces of the pharynx are of cellular or vacuolar nature, although no nucleus has been observed within. *s*, syncytium. **f** Detail of muscle myofibrills nearby the opening of the pharynx, where muscle fibers are thicker. **g** Detail of a cell of the pharynx envelope, nearby the opening of the pharynx. The cytoplasm is very rich in endoplasmic reticulum sacs, suggesting a secretory function. **h** Detail of the epithelial cells nearby the pharynx opening, heavily ciliated. The epithelial vertical profile is thicker here than elsewhere in the primary epidermis. *Bottom* is outside. **i** Detail of **h**. A large junction along both contiguous epithelial cells is shown (*arrowheads*). The basal membrane of these epithelial cells presents several invaginations and projections (*arrow*), suggesting some direct relationship between these surface cells and the underlying pharyngeal cells. *Scale bar* 100 μm in **b**, 1 μm in **f**

Star cells

Stage 2 embryos possess a small number of large, multipolar cells which we named star cells (Cardona et al. 2005a). Star cells are located in between the primary epidermis and the yolk syncytium and are labeled by acTub, tyrTub, and anti-serotonin (Fig. 7a–c). A star cell typically possesses one thick cytoplasmic process and three thin processes (Fig. 7b,c). These processes extend parallel to the primary epidermis and appear to contact blastomeres (Fig. 7b). The thick process is rich in microtubules and lies very close to the primary epidermis; it may represent a sensory structure (Fig. 7c) similar to the ones found in early neurons of snail embryos (Diefenbach et al. 1998).

As the embryonic pharynx starts imbibing external yolk, thereby generating an inner gastric cavity within the cryptic larva (stage 3), star cells can no longer be detected below the primary epidermis. Several multipolar cells can instead be found deeper inside the embryo (Fig. 7d–g; Cardona et al. 2005a). The cell bodies of these late star cells lie on the lateral sides of the embryo within the space formed by the gastric cavity, and their processes extend over the inner syncytial membrane, in close contact to the imbibed yolk cells (Fig. 7e–g). The branching pattern of these cells is also quite different from stage 2 star cells: each late star cell possesses more than 20 thin processes which radiate over a larger area than earlier star cells did. The area permeated by the processes of a single late star cells can cover as much as half of the embryo (Cardona et al. 2005a). Late star cells also lack the distinctive thick process characteristic of early star cells.

It is tempting to speculate that the star cells represent a primitive nervous system of the cryptic larva that is able to modulate its motility and feeding behavior. In an attempt to obtain more information about the possible function of star cells, we have labeled stage 3/4 embryos with more than 30 different commercially available antibodies, with no success (Cardona 2005). Thus, the only markers found so far to be expressed in star cells are acTub, tyrTub, and anti-serotonin. Given that both muscle cells and many neurons immunoreact with tyrTub in later planarian embryos (Cardona et al. 2005a), there is little support for the conclusive classification of star cells as either muscle or nerve cells.

Discussion

This paper focuses on the early stages of embryonic development in planarians. After the formation of a yolk syncytium, cleavage produces two populations of blastomeres. One population differentiates into the body of a

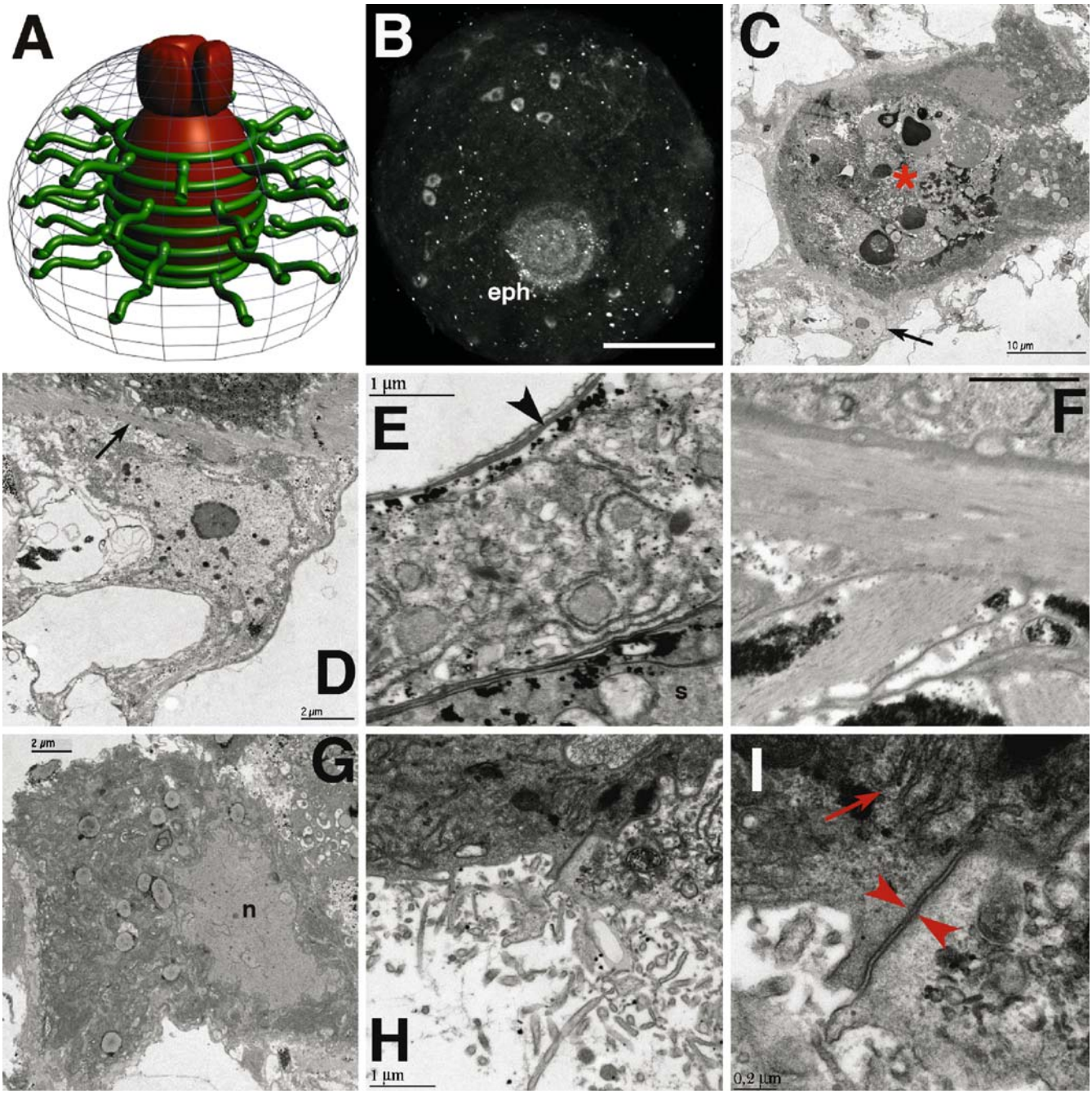

cryptic larva that forms around the syncytium; the other population keeps dividing within the syncytium and gives rise to the embryonic cells that eventually replace the tissues of the cryptic larva and form the body of the juvenile worm. We have analyzed the structure of the cryptic larva and the events that lead up to the formation of this peculiar organism.

Origin and function of yolk cells

Confirming the descriptions of previous authors (le Moigne 1963; Marinelli and Vagnetti 1973; Gremigni and Domenici 1974), we identified two types of yolk cells in eggs at around the stage when cleavage begins: large and lipid-rich spherical yolk cells and motile, RNA-rich fusiform yolk cells. The latter type aggregates around the cleaving zygotes and forms the yolk syncytium that surrounds the early embryo. The classical theories concerning syncytium formation by means of yolk cell fusion state that spherical yolk cells respond to zygote-released signals and transform into spindle-shaped yolk cells which then fuse (Seilern-Aspang 1958). Koscielski (1966) described that spherical yolk cells falling within a certain perimeter around the zygote become spindle-shaped and polarized, accumulating mitochondria and RNA at the cell pole facing the zygote. The spindle-shaped yolk cells subsequently fuse around the zygote,

encapsulating it in a syncytial mass. While our data agree with the notion of fusiform yolk cells forming the syncytium, the pattern in which these cells appear in the first place is different from what has been reported previously. Thus, fusiform yolk cells occur ubiquitously in the egg capsule and are not restricted to the immediate neighborhood of the zygotes. This observation is further supported by the formation of fusiform yolk cells in vitro, without any close-by zygote. We conclude that if the transformation of yolk cells from spherical to fusiform were induced by the zygote, the range of the signals must exceed the 70 μm reported by Koscielski (1966).

It has been reported that the yolk nuclei inhabiting the syncytium undergo karyorrhexis (Koscielski 1966). Our findings agree with this observation, although the time at which yolk nuclei disappear is considerably later than previously thought. Thus, many (if not all) syncytial nuclei retain their characteristic corona of electron-dense cytoplasm and undergo nuclear division in a synchronous fashion. The time at which yolk nuclei finally disappear coincides with the differentiation of the blastomere-derived embryonic cells forming the epidermis, musculature, and nervous system of the juvenile body (stage 5). During the stages of cleavage, syncytial yolk nuclei are very abundant (more than 300 in a late stage 2 embryo) and are spread out throughout the syncytium. It is quite likely that these maternally derived nuclei, along with the organelles and RNA contained within the syncytial cytoplasm, could play a fundamental role in providing maternal determinants and morphogens that control early embryogenesis. Such a role would go far beyond the traditional function of yolk as a source of nutrients (glycogen and yolk granules) and the cytoplasmic organelles for nutrient processing.

A close relationship between maternal cells and zygotically derived embryonic cells has also been reported for *Hydra*. In this organism, nurse cells are phagocytosed by the oocyte and then remain within vacuoles without completing apoptosis until the polyp hatches (Technau et al. 2003). Nurse cells remarkably undergo apoptosis in a particular time sequence that is appropriate for oocyte development. It may be therefore no mere coincidence that in triclads, yolk nuclei and the surrounding sycytial yolk cytoplasm is reabsorbed at the stage when widespread differentiation of embryonic cells occurs (stage 5; le Moigne 1963, 1966; Cardona et al. 2005a).

Blastomeres

In contrast to syncytial yolk nuclei, the increase in number of blastomeres is slow at the beginning of development (stages 2 and 3). Besides those forming the tissues of the cryptic larva, only 15–20 cells can be identified in a late stage 2 embryo. The massive allocation of embryonic resources to tissues of the cryptic larva, which provides a unique vehicle for yolk cell acquisition (embryonic pharynx and primary epidermis), could explain the lag phase of blastomere cleavage during stages 2 and 3.

Planarian blastomeres are not attached to each other. Any communication between these cells must be mediated by the syncytium, possibly by gap junctions between the blastomeres and the syncytium itself (Fig. 3d). As blastomeres undergo mitosis, the ‘vacuoles’ in which they are contained enlarge. Reservoir materials must be assumed to cross the double membrane between syncytium and blastomere by means of specific receptors and channels. This transport may explain the presence of a microfilament network containing numerous mitochondria lining the syncytial side of the vacuole membrane (Fig. 3i).

The presence of the dense cytoplasmic corona and, in some cases, membrane bound clefts around the syncytial yolk nuclei, not to mention the fact that they undergo frequent mitoses, prompted us to classify some of these yolk nuclei as a separate group of blastomeres (type 2 blastomeres; Cardona et al. 2005a). However, electron micrographs show that the corona of syncytial yolk nuclei morphologically corresponds to that of fusiform yolk cells before their fusion; furthermore, a double membrane around the corona, which would indicate that it represents a separate cell enclosed within the syncytium, is absent. These observations lead us to discard the nomenclature of type 1 and type 2 blastomeres.

Primary epidermis and epidermal succession

Based on Skaer (1965) and Sakurai and Ishii (1995) data, Tyler and Tyler (1997) proposed a model of epidermal succession in triclads that would closely match that of parasitic platyhelminthes except for the formation of a neodermis. According to this model, epidermal development begins with the formation of a syncytial, non-ciliated primary epidermis. In more derived taxa (e.g., rhabdocoels and neodermata), this primary epidermis is reduced to a thin membrane called hull membrane. The primary epidermis/hull membrane is followed by a secondary epidermis, whereby embryonic cells that start to differentiate underneath the primary layer insert themselves into the primary epidermis. The secondary epidermis is later replaced by a third wave of epidermal precursors that, like secondary cells did earlier, differentiate subepidermally before intercalating into the secondary epidermis.

Our data show that a complete, cellular, ciliated (primary) epidermis forms around the cryptic larva by the end of stage 2. It is possible that the previous authors (Sakurai and Ishii 1995; Tyler and Tyler 1997) only investigated early stages that preceded primary epidermal differentiation (i.e., ciliation). It is also unlikely that the primary epidermis of triclads can be compared to the hull membrane of a rhabdocoel. The rhabdocoel hull membrane is formed by yolk cells (Hartenstein and Ehlers 2000) and does indeed not possess cilia. It is much more likely that the structure we describe as hull membrane in this paper corresponds to the hull membrane of rhabdocoels. It is also formed by yolk cells, is most likely syncytial, and is definitively devoid of cilia. Previous works on triclad embryonic ultrastructure had not explicitly mentioned the

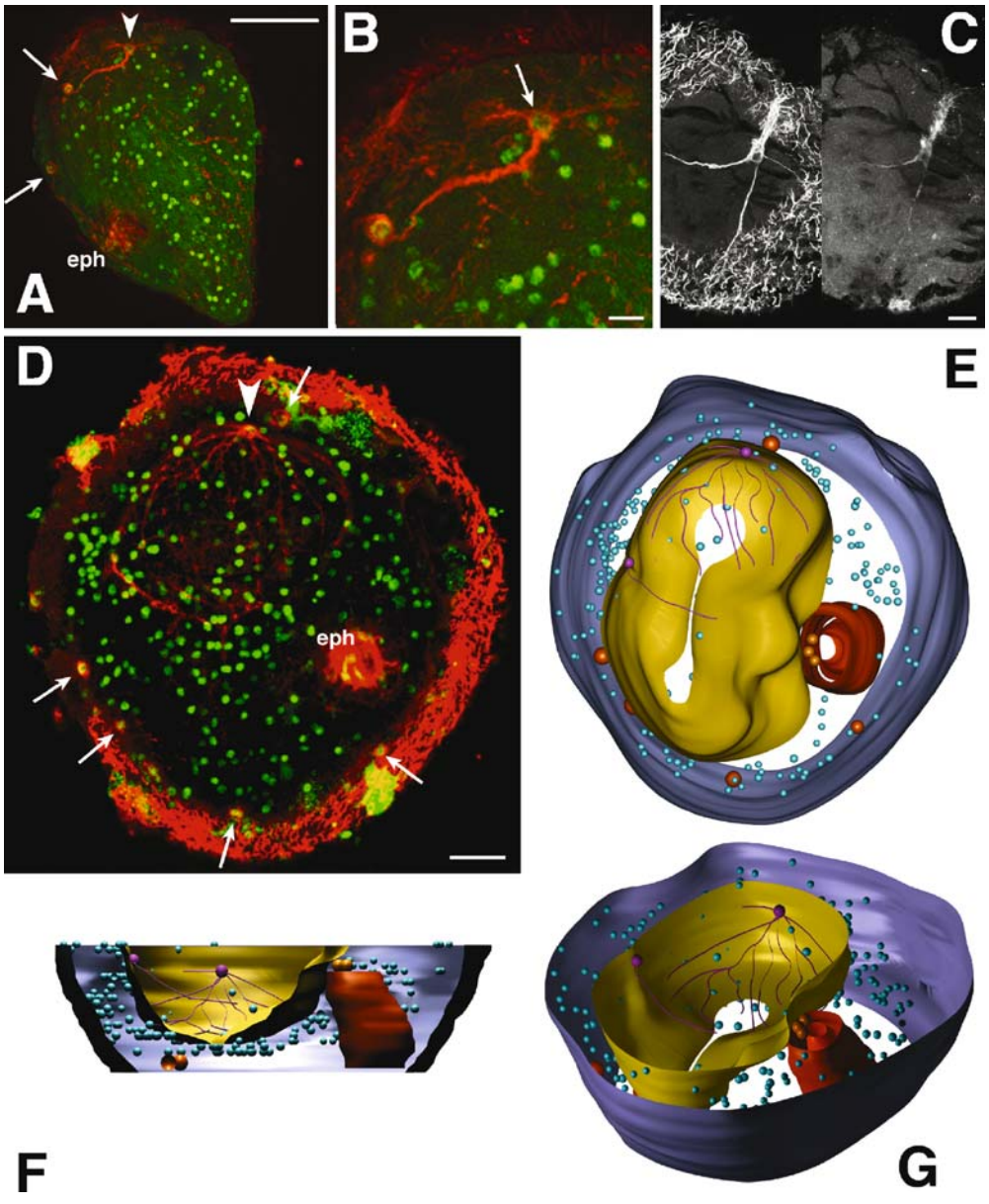

Fig. 7 Star cells. Panels **a**–**c**, stage 2. Panels **d**–**g**, stage 3. **a**, **b** Panels show confocal z-projections of tyrTub (*red*) whole-mount antibody labelings; nuclei labeled with Sytox (*green*). **c** Panel shows a confocal z-projection of a whole-mount double antibody labeling: acTub (*left*) and anti-serotonin (*right*). **d** Confocal z-projection of a whole-mount antibody labeling with acTub; nuclei labeled with Sytox (*green*). **e**–**g** Panels show 3D models based on the confocal stack shown in **e**. **a** Stage 2 embryo. Star cells (*arrowhead*) are always located far from the developing embryonic pharynx (*eph*). Two blastomeres are visible (*arrows*). The whole embryo is sparsely ciliated (cilia in *red*). **b** High magnification of star cell in **a** (*arrowhead* cell body). Note the typical three thin branches and the thicker fourth, the latter contacting a blastomere (*lower left*). **c** Star cell double-labeled with acTub (*left*) and anti-serotonin (*right*). For the *left panel*, top five confocal sections were not included in the z-projection to prevent the ciliation signal from masking the underlying star cell. Note that the anti-serotonin signal is not due to channel bleeding as the strong signal of cilia (*left*) is not present in the anti-serotonin channel (*right*). **d** Stage 3 embryo featuring a highly branched star cell (*arrowhead* cell body), wrapping the contents of the gastric cavity (no boundaries visible). Blastomeres are present within the peripheral rind of syncytium (*arrows*). **e**–**g** Dorsal (**e**), lateral (**f**), and perspective (**g**) views of a stage 3 embryo. The embryonic pharynx (*large red structure*) sits at a posterior–ventral position and provides directionality to the embryo. A star cell (*branched purple cell*) lays typically on both lateral sides of the embryo (one side shown only) and extends its projections close to the gastric cavity perimeter (*yellow*). Blastomeres (*large red spheres*), very scarce, and syncytial yolk nuclei (*small blue spheres*), very abundant, coexist within the syncytium (*space* between the epidermis in *purple* and the gastric cavity perimeter in *yellow*). *Scale bar* 100 μm in **a**, **d** and 10 μm in **b**, **c**

hull membrane, although some of the figures (Fig. 1 in Seilern-Aspang 1958) suggest its presence.

Star cells: a novel type of transient neurons?

Star cells represent a very particular cellular type of the early triclad embryos. Early star cells, immunoreactive to

anti-serotonin, tyrTub, and acTub and presenting a thick tubulin-rich branch, could be of a sensorial type. There have not been any descriptions of such or similar cellular types in the homologous stages of development of other platyhelminthes, but early embryonic neuronal cells (ENC1) in the snail *Lymnaea stagnalis* have been reported to use 5-HT as the neurotransmitter of choice (Diefenbach et al. 1998). These cells innervate the ciliary bands of the snail trochophora larva and, similarly to planarian star cells, they present one or two short neurites and a much longer, thicker neurite.

While stage 2 embryos of triclads do not display any ciliary bands or tufts, they are indeed ciliated (Fig. 6g–i). Furthermore, cilia motility of the stage 2 embryo has been observed in vitro on cultured stage 2 embryos, under the microscope. The presence of 5-HT-containing star cells underneath a ciliated epidermis suggests a similar relationship as that of ENC1 cells in the snail larva. The evident polarization of star cells, which present one thick branch in close contact to the surface and three thinner, longer ones (Fig. 7a–c), suggests a sensorimotor function. We hypothesize that the early star cells could have a role as cilioexcitatory motor neurons during embryonic development, in a similar fashion to the ENC1 of snails (Koss et al. 2003). In the present scenario, there is little data to conclude whether the early and late start cells constitute a single or two separate types of cells.

The cryptic larva in the embryonic development of triclads

We can envisage two evolutionary mechanisms by which early triclad embryos could have acquired the aforementioned larval features: (1) the cryptic larva is a vestigial larval form that has evolved from a true larva present in the ancestral triclad and (2) the constraints imparted on the developing triclad by the presence of multiple embryos in direct competition for maternal resources could favor the precocious adoption of an active motile and feeding life style.

In line with the first hypothesis, it can be stated that the evolution of cryptic larvae from normal larvae is observed in many animal groups. An example is presented by the Tse-Tse fly whose larva remains within the egg capsule from which it finally hatches as a full-featured, winged adult (Jordan 1993). Phylogenetically closer to triclads and therefore perhaps more relevant, several species of polyclads that develop their Goette's larva within the egg capsule (Kato 1940) might be considered. One might view the presence of a cryptic larva, devolving from a free-living larval or juvenile form, in the context of the evolution of ectolecithy. Triclads belong to one of the most basal (if not the most basal) flatworm clades that are ectolecithal. One might envisage a scenario in which triclad ancestors had not yet evolved an ectolecithal mode of development. Mature embryos hatched as larvae or juveniles. After the "invention" of an ectolecithy, the mature embryos ready to hatch found themselves surrounded by a thick yolk mantle. This provided an opportunity for these embryos to change their mode of development. Rather than all tissues differentiating simultaneously, leading up to a juvenile/larva that could cope with an external environment, only a small subset of cells assemble into a simple organism (the cryptic larva) that ingests the external yolk, whilst other cells developed slowly within the body of the cryptic larva.

According to the second hypothesis, the cryptic larva is an adaptation to the particular competition presented by the presence of multiple embryos in one nutrient-rich, ectolecithal egg. Rather than devolving from a true larva/juvenile in the triclad ancestor, the cryptic larva would evolve from a "regular" type of embryo such as the one found in other ectolecithal flatworms (rhabdocoels; Giesa 1966; Rieger et al. 1991). The standard rhabdocoel embryo forms a multilayered disc ("embryonic primordium") embedded in the massive maternally derived yolk mantle. After proliferation, the cells at one side of the disc differentiate as the epidermal layer that expands on all sides and grows around the yolk (Hartenstein and Ehlers 2000); Younossi-Hartenstein and Hartenstein 2001).

The novelty that could have prompted the evolution of a motile cryptic larva from a regular, non-motile embryo (such as the one found in rhabdocoels) could be the occurrence of multiple embryos in a single egg. The fact that a limited amount of resources is shared by several co-developing embryos may be the basis for positive selection of genotypes that are fastest and most efficient in acquiring maternal resources (i.e., unfused vitellocytes). The genomic competition aspect is emphasized by the fact that co-developing embryos are on average each from a different father and thus share only 25% of the variable part of the genome with each other (Pongratz et al. 2002). We hypothesize that the delay in juvenile tissue formation and the precocious appearance of an embryonic pharynx and other differentiated tissues of the cryptic larva could be the outcome of such a selection.

Acknowledgements The authors wish to express their gratitude to Núria Cortadellas and Almudena Fernández from the Serveis Científico-Técnics UB for their exquisite professional expertise in electron microscopy, to Juani Fernandez-Rodriguez for sharing her expertise in generating and hybridizing *myoD* probes, and also to Cati Lee for laboratory assistance in sequencing and synthesizing the probes. The authors are deeply thankful for extensive and encouraging comments from the anonymous reviewers. AC was supported by an FPU fellowship from the MEC, Spain. This work was supported by grants NIH NS29367 and NSF to IBN-0110718 to VH and BFU2004-05015 from the PNIC-DIT 2004-07 by the MEC, Spain to RR. Many thanks to Lukas Schärer and the Institute of Zoology in Innsbruck for extremely helpful discussions.

References

Auladell C, Valero JG, Baguna J (1993) Ultrastructural localization of RNA in the chromatoid bodies of undifferentiated cells (neoblasts) in planarians by the Rnase-Gold complex technique. J Morphol 216:319–326

Baguna J, Riutort M (2004). Molecular phylogeny of the platyhelminthes. Can J Zool 82(2):168–193

Benazzi M, Gremigni V (1982) Developmental biology of triclad turbellarians (*Planaria*). In: Liss AR (ed) Developmental biology of freshwater invertebrates. New York, pp 151–211

Bueno D, Baguna J, Romero R (1997) Cell-, tissue-, and position-specific monoclonal antibodies against the planarian *Dugesia* (*Girardia*) *tigrina*. Histochem Cell Biol 107(2):139–149

Bueno D, Fernandez-Rodriguez J, Cardona A, Hernandez-Hernandez V, Romero R (2002) A novel invertebrate trophic factor related to invertebrate neurotrophins is involved in planarian body regional survival and asexual reproduction. Dev Biol 252(2):188–201

Cardona A (2005) The embryonic development of the planarian *Schmidtea polychroa* using molecular markers. Ph.D. thesis, University of Barcelona

Cardona A, Hartenstein V, Romero R (2005a) The embryonic development of the triclad *Schmidtea polychroa*. Dev Genes Evol 215(3):109–131

Cardona A, Fernandez-Rodriguez J, Solana J, Romero R (2005b) An in situ hybridization protocol for planarian embryos: monitoring myosin heavy chain gene expression. Dev Genes Evol 215(9):482–488

Cebrià F (2000) DeterminaciÚ, diferen ciaci i restituciÚ del patrÚ muscular durant la regeneraciÚ i renovaciÚ cel.lular a plan‡ries d'aigua dolÁa. Ph.D. thesis, University of Barcelona

Diefenbach T, Koss R, Goldberg J (1998) Early development of an identified serotoninergic neuron in *Helisoma trivolvis* embryos: serotonin expression, de-expression, and uptake. J Neurobiol 34(4):361–376

Domenici L, Gremigni V (1974) Electron microscopical and cytochemical study of vitelline cells in the fresh-water triclad *Dugesia lugubris* s.l. II. Origin and distribution of reserve materials. Cell Tissue Res 152(2):219–228

Fulinski B (1916) Die KeimblÇtterbildung bei *Dendrocoelum lacteum* Oerst. Zool Anz 47:380–400

Giesa S (1966) Die embryonalentwicklung von *Monocelis fusca* Oersted. Z Morphol Okol Tiere 57:137–230

Gremigni V, Domenici L (1974) Electron microscopical and cytochemical study of vitelline cells in the fresh water triclad *Dugesia lugrubris* s.l. I. Origin and morphogenesis of cocoon-shell globules. Cell Tissue Res 150(2):261–270

Hartenstein V, Ehlers U (2000) The embryonic development of the rhabdocoel flatworm *Mesostoma lingua*. Dev Genes Evol 210:399–415

Jordan A (1993) Tsetseflies (Glossinidae). In: Lane R, Crosskey R (eds) Medical insects and arachnids, chapter 9. Chapman & Hall, London

Kato K (1940) On the development of some Japanese polyclads. Jpn J Zool 8:537–573

Koscielski B (1966) Cytological and cytochemical investigations on the embryonic development of *Dendrocoelum lacteum* O.F. M∏ller. Zool Pol 16(1):83–102

Koss R, Diefenbach T, Kuang S, Doran S, Goldberg J (2003) Coordinated development of identified serotoninergic neurons and their target ciliary cells in *Helisoma trivolvis* embryos. J Comp Neurol 457(4):313–325

le Moigne A (1963) Etude du dèveloppement embryonnaire de *Polycelis nigra* (Turbellariè, Triclade). Bull Soc Zool Fr 88:403–422

le Moigne A (1966) Etude du dèveloppement embryonaire et recherches sur les cellules de la règènèration chez l'embryon de la Planaire *Polycelis nigra* (Turbellariè, Triclade). J Embryol Exp Morphol 15:39–60

le Moigne A (1969) Étude dy développement et de la régénération embryonnaires de *Polycelis nigra* (Ehr.) et *Polycelis tenius* (lijima) turbellaries triclades. Anal d'Embr Morph 2(1):51–69

Marinelli M, Vagnetti D (1973) Electron microscopic investigations on the yolk cells in the cocoon of *Dugesia lugubris* s.l. Boll Zool 40:367–369

Orii H, Sakurai T, Watanabe K (2005) Distribution of the stem cells (neoblasts) in the planarian *Dugesia japonica*. Dev Genes Evol 205(3):143–157

Pongratz N, Gerace L, Michiels N (2002) Genetic differentiation within and between populations of a hermaphroditic freshwater planarian. Heredity 89(1):64–69

Rasband W (1997–2006) ImageJ. http://www.rsb.info.nih.gov/ij/

Reddien PW, Bermange AL, Murfitt KJ, Jennings JR, Sanchez Alvarado A (2005) Identification of genes needed for regeneration, stem cell function, and tissue homeostasis by systematic gene perturbation in planaria. Dev Cell 8(5):635–649

Rieger R, Tyler S, III JS, Rieger G (1991) Platyhelminthes: Turbellaria. In: Harrison F, Bogitsh B (eds) Platyhelminthes and Nemertinea. Microscopic anatomy of invertebrates, vol 3, chapter 2. Wiley-Liss, New York, pp 7–140

Sanchez-Alvarado A (2003) The freshwater planarian *Schmidtea mediterranea*: embryogenesis, stem cells and regeneration. Curr Opin Genet Dev 13(4):438–444

Sanchez Alvarado A, Newmark PA (1999) Double-stranded RNA specifically disrupts gene expression during planarian regeneration. Proc Natl Acad Sci USA 96:5049–5054

Sakurai T, Ishii S (1995) An ultrastructural study of primary epidermis formation in *Bdellocephala brunnea* (Turbellaria; Tricladida). Invertebr Reprod Dev 28:77–85

Seilern-Aspang F (1958) Entwicklungsgeschichtliche studien en paludicolen tricladen. Roux' Archiv f∏r Entwicklungsmechanik 150:425–480

Skaer R (1965) The origin and continuous replacement of epidermal cells in the planarian *Polycelis tenuis* (Ijima). J Embryol Exp Morphol 13:129–139

Shibata N, Umesono Y, Orii H, Sakurai T, Watanabe K, Agata K (1999) Expression of vasa(vas)-related genes in germline cells and totipotent somatic stem cells of planarians. Dev Biol 206 (1):73–87

Stevens M (1904) On the germ cells and the embryology of *Planaria simplissima*. Proc Natl Acad Sci Phila 56:208–220

Technau U, Miller M, Bridge D, Steele R (2003) Arrested apoptosis of nurse cells during *Hydra* oogenesis and embryogenesis. Dev Biol 260:191–206

Thomas M (1986) Embryology of the Turbellaria and its phylogenetic significance. Hydrobiologia 132:105–115

Tyler S, Tyler M (1997) Origin of the epidermis in parasitic platyhelminths. Int J Parasitol 27(6):715–738

Umesono Y, Watanabe K, Agata K (1997) A planarian orthopedia homolog is speci?cally expressed in the branch region of both mature and regenerating brain. Dev Growth Differ 39(6):723–727

Younossi-Hartenstein A, Hartenstein V (2001) The embryonic development of the temnocephalid flatworms *Craspedella pedum* and *Diceratocephala sp*. Cell Tissue Res 304:295–310